

A Review on Drag Reduction Methods of Ahmed Body at Different Rear Slant Angles using Computational Fluid Dynamics Approach

Ambar Shrivastava¹, Anandrao Jaurker²

¹ PG Student, Department of Mechanical Engineering, Jabalpur Engineering College, Jabalpur, 482011, Madhya Pradesh, India.

² Professor, Department of Mechanical Engineering, Jabalpur Engineering College, Jabalpur, 482011, Madhya Pradesh, India.

Abstract - The steering stability, efficiency, convenience, and safety of an automobile are all influenced by the vehicle's aerodynamic properties. A vehicle with minimal drag resistance has an added benefit in value for money and performance. The aerodynamic drag of vehicles can be reduced by employing shape optimization and ADD-ON devices. Different types of aerodynamics ADD-ON devices (i.e., vortex generators, diffusers, wings, spoilers etc.) are used to reduce the drag of a vehicle. The recent advancement of computational fluid-dynamic technology allows predicting air flows around a vehicle that is exceptionally close to its actual condition. In this review paper, Ahmed body which is simplified generic vehicle geometry is reviewed with the application of various aerodynamic devices for drag reduction using the numerical methodology. Square back and Hatchback configuration of Ahmed body with rear slant angles of 0° , 25° , and 35° are considered in this study.

Key Words: Drag coefficient, Drag reduction, Computational fluid dynamics, Ahmed body, Rear slant angles, Aerodynamic ADD-ON devices.

1. INTRODUCTION

1.1 Aerodynamic Drag

Aerodynamic drag [1] is a force operating in the opposite direction of any object moving relative to air. Two significant components of drag force are pressure and skin friction force. Pressure drag dominates ground vehicle aerodynamics, whereas skin friction drag dominates aircraft and marine ships. The basic formula of aerodynamic drag force is given in equation (i).

$$F_{\text{Aerodynamic Drag}} = 0.5C_d\rho Av^2 \quad \text{eq. (i)}$$

Where,

C_d = Coefficient of Drag

ρ = Air density (in kg/m^3)

A = Frontal area (in m^2)

v = Relative velocity of object w.r.t. air medium (in m/s)

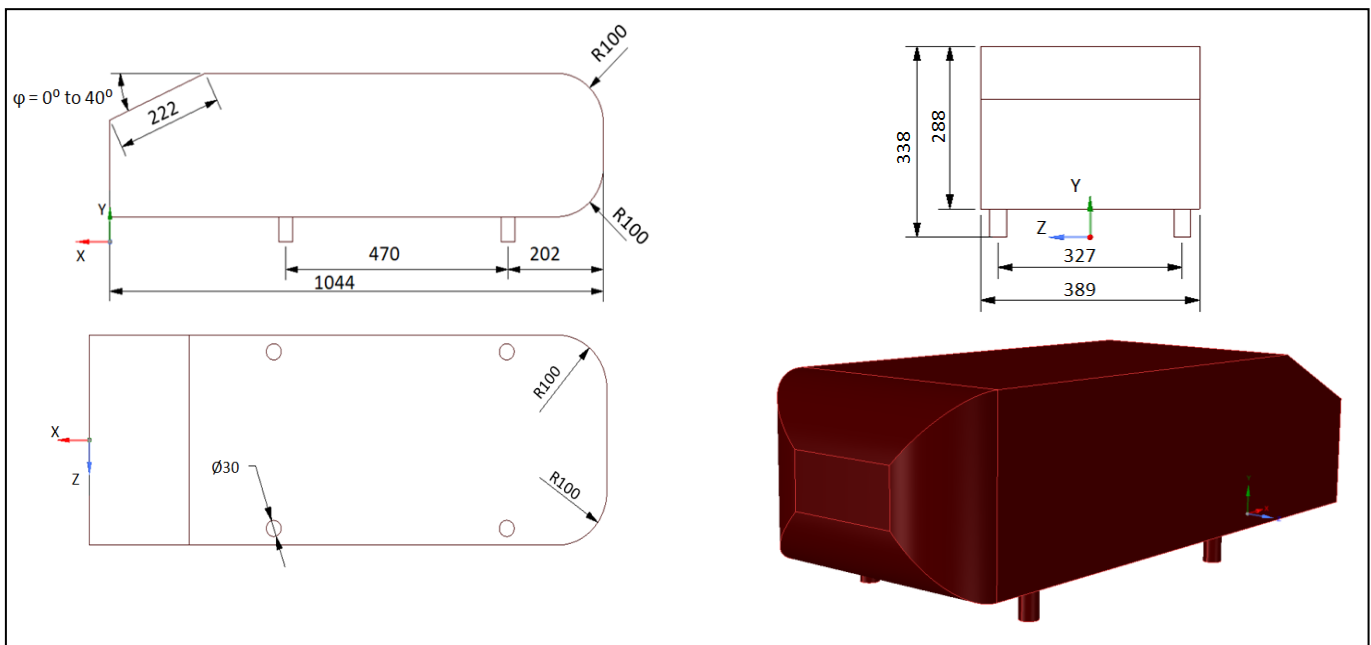


Fig - 1: Dimensions of Ahmed Body with 3D model [2].

1.2 Ahmed Body

Ahmed Body is a simplified vehicle model, which is a rectangular box mounted on four legs whose front edges are rounded, and the rear slant end is adjustable to study the flow detachment at angles from 0° to 40°. Dimensions of Ahmed body are shown in fig-1. Ahmed body is about a quarter of an actual automobile (i.e., hatchback, sedan, and others) whose experimental data are used to validate the actual vehicle's experimental and computational aerodynamic results. **Ahmed et al. (1984)** [3] experimentally concluded that the total drag on the Ahmed body was dominated by pressure drag of about 85%, while friction drag accounted for the remaining. Furthermore, the rear end generated most of the pressure drag of about 91%, while the frontal portion was responsible for the remaining drag. The magnitude of pressure drag generated at the rear end was highly dependent on the Rear Slant Angle (φ). In this review paper, Ahmed body for Square-back (with $\varphi = 0^\circ$) and Hatchbacks (with $\varphi = 25^\circ$ and 35°) are considered for the study. In addition, various types of aerodynamic drag devices or ADD-ONS used in previous numerical studies for the drag reduction of Ahmed body are reviewed in the literature study section.

1.3 Computational Fluid Dynamics

“Computational fluid dynamics (CFD)” is a branch of continuum mechanics concerned with fluid flow and heat transport issues numerical modeling. Core mathematical equations, usually in the partial differential form that governs a process of importance and are referred to as governing equations in CFD, may usually be utilized to define the physical characteristics of fluid motion. It combines not just fluid mechanics and mathematics but also computer science [4].

Highly turbulent, three-dimensional separations define the flow around vehicles. As a result, the demand for powerful numerical methods to analyze them rises. CFD based on “Reynolds-Averaged Navier-Stokes Equations (RANS)”, “Large Eddy Simulation (LES)”, and other turbulence models is commonly used in the automobile industry. Somewhat of using individual point measurements taken from a wind tunnel investigation, CFD gives continuous and precise flow visualization of aerodynamic characteristics over the whole surface regions of the vehicle [5]. From this information, flow separation, recirculation bubbles can be retrieved, as shown in fig-2, fig-3, and fig- 4 for Ahmed body with $\varphi = 0^\circ$, 25° , and 35° , respectively.

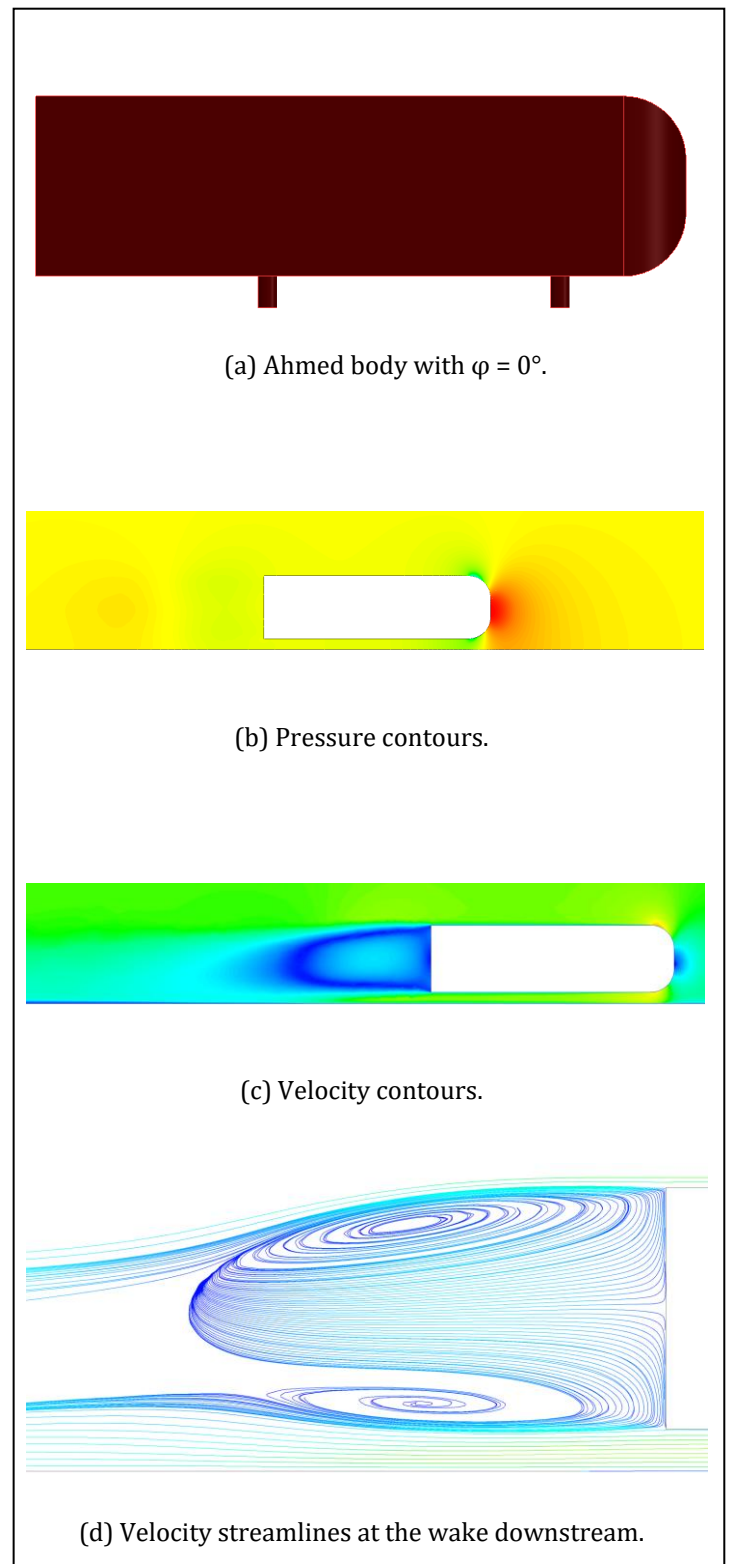


Fig – 2: CFD flow predictions of Ahmed body with $\varphi = 0^\circ$.

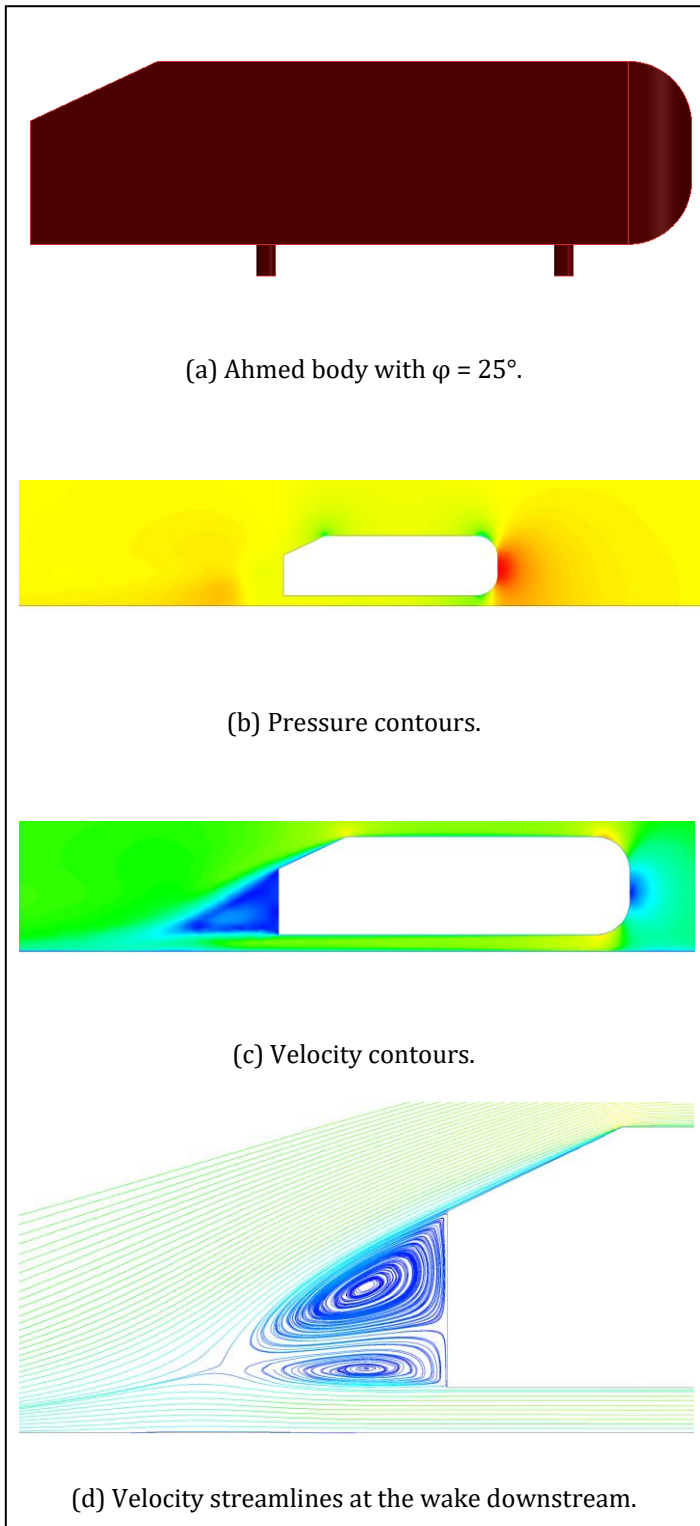


Fig - 3: CFD flow predictions of Ahmed body with $\varphi = 25^\circ$.

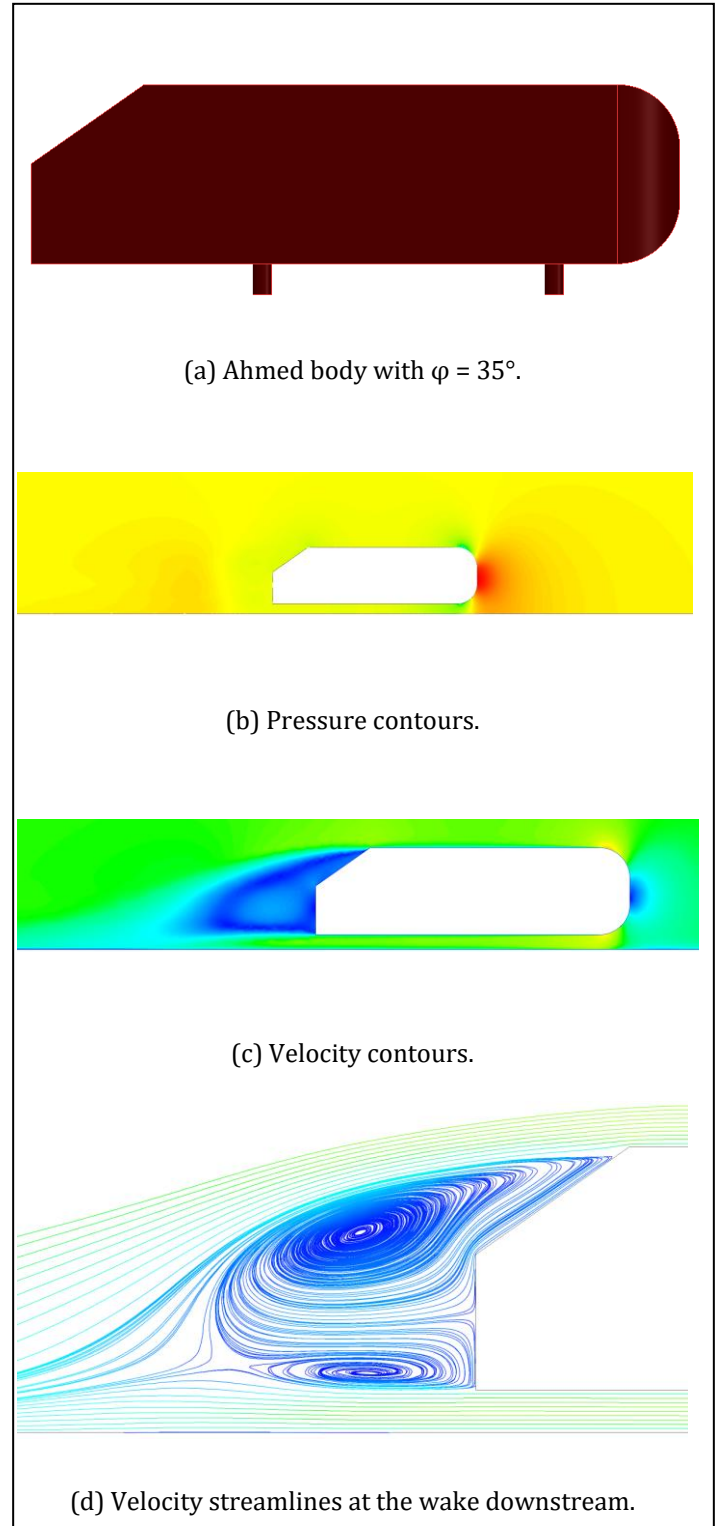


Fig - 4: CFD flow predictions of Ahmed body with $\varphi = 35^\circ$.

2. LITERATURE STUDY

Bruneau et al. (2008) [6] numerically studied the effect of porous devices added at different locations on a two-dimensional Ahmed Body with $\phi = 0^\circ$ (i.e., for square-back). Simulations were analyzed for two conditions: on top of a road and in an open domain (without a road). A total of eight scenarios were modeled for analysis. Baseline Ahmed body (without porous layer) was taken as scenario 0. The modified models in the form of seven scenarios used in their paper are given below:

- Scenario 1 - Ahmed body with a porous layer at the top rounded corner part of the front section.
- Scenario 2 - porous slice in the entire top of Ahmed body.
- Scenario 3 - it was symmetrical to scenario 1.
- Scenario 4 - it was symmetrical to scenario 2.
- Scenario 5 - same as scenario 4 with the inclusion of the front section.
- Scenario 6 - same as scenario 5 with the inclusion of the back section.
- Scenario 7 - porous layers of scenario 6 were removed, resulting in a shorter Ahmed body.

Of the scenarios mentioned above, scenario 2 was the best, with a maximum drag reduction of 45%.

Abdul Latif et al. (2019) [7] performed the drag reduction simulation on a simplified generic vehicle model by adding the dimple grid based on a golf ball at the top at various locations to study boundary layer flow separation.

- The goal of their study was to assist a local Malaysian bus manufacturer in lowering the fuel consumption of each bus by installing the drag Reduction devices.
- Ahmed Body with $\phi = 0^\circ$, closely resembling a bus body, was taken as the baseline model for aerodynamic analysis. CATIA V5R21 was used for CAD modeling. The simulation was conducted in AcuSolve, the CFD software, via Spalart Allmaras's turbulence model.
- The design of the Experiment technique was used to optimize the dimple grid in which sixteen combinations were obtained based on four variables. The normal plot, half-normal plot, and Pareto chart were analyzed to get the best model with a desirability value nearest to 1.
- Pressure contours, velocity contours, and streamline were generated for flow visualization, and good results were found.
- Drag reduction of 36.5% was found by applying an optimized golf ball based dimple grid.

Finally, the work was concluded with a fuel consumption calculation with a fuel consumption reduction of 18.54% based on the aerodynamic drag.

Yang et al. (2022) [8] analyzed the baseline model (Ahmed Body with $\phi = 25^\circ$). ANSYS FLUENT, CFD software was used for simulation via "Improved Delayed Detached Eddy Simulation" (IDDES) for drag reduction by adding two different ADD-ONS, first: an array of Vortex Generators (VGs) of new type "Hemispherical Round Roughness Elements" to rear and slant end of Ahmed body and second: Riblets of V-shape to rear and slant end of Ahmed body. Both the ADD-ONS were analyzed individually and by making the various combinations of them, whose percentage drag coefficients result, are given in table 1.

Table- 1: Drag coefficient reduction in (%) w.r.t to baseline Ahmed body.

S. No.	Configurations	Drag coefficient reduction
1	VGs attached to the rear surface	6.21%
2	VGs attached to the slant surface	4.37%
3	V-Shaped Riblets attached to the rear surface	3.03%
4	V-Shaped Riblets attached to slant surface	2.21%
5	VGs attached on both rear and slant surfaces	7.76%
6	V-shaped Riblets attached on both rear and slant surfaces	3.41%
7	VGs attached on rear surfaces and V-shaped Riblets attached on slant surfaces	4.38%
8	VGs attached on slant surfaces and V-shaped Riblets attached on rear surfaces	8.62%

Out of the results mentioned above, the combination of VGs attached on slant surfaces and V-shaped Riblets attached on rear surfaces was the best configuration, with a drag coefficient reduction of 8.62%.

Tian et al. (2017) [9] numerically investigated the novel ADD-ON device for two models of Ahmed body (i.e., with rear slant angles of 25° and 35°). Two types of flaps (i.e., "big-type" and "small-type" were added on the top, side and bottom edges of slant surfaces (see fig-5) of both the models of Ahmed body for analysis of aerodynamic drag. Simulations were carried out on STAR-CCM+, the CFD software via RANS based SST k-omega turbulence model at a Reynolds number of 4.29 million. Drag reduction was prominent for Ahmed body with 25° , whose results are shown in fig – 6. Various cases were made for the analysis of the flap for Ahmed body with $\phi = 25^\circ$ (i.e., "Top_small_40, Top_big_20, Side_big_80, and Bottom_big_130" etc.) at different flap angles (α) in which Side_big_80 shows the highest drag reduction of 21%. Furthermore, Ahmed body with a rear slant angle of 35° shows a drag of 6% only.

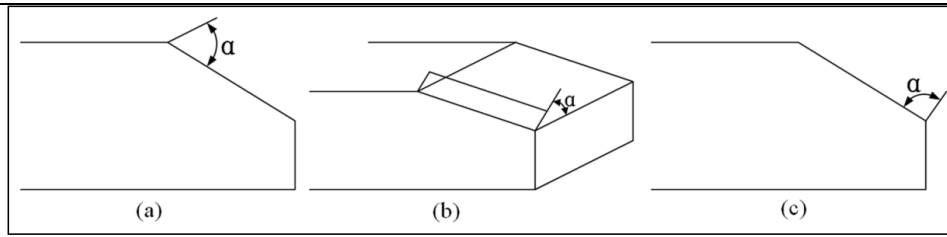
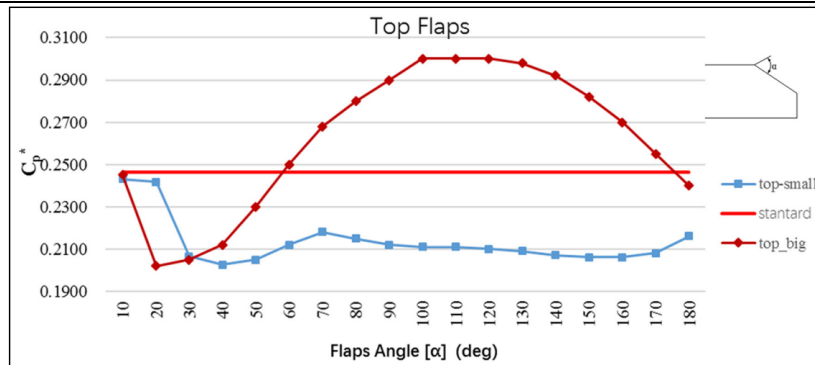
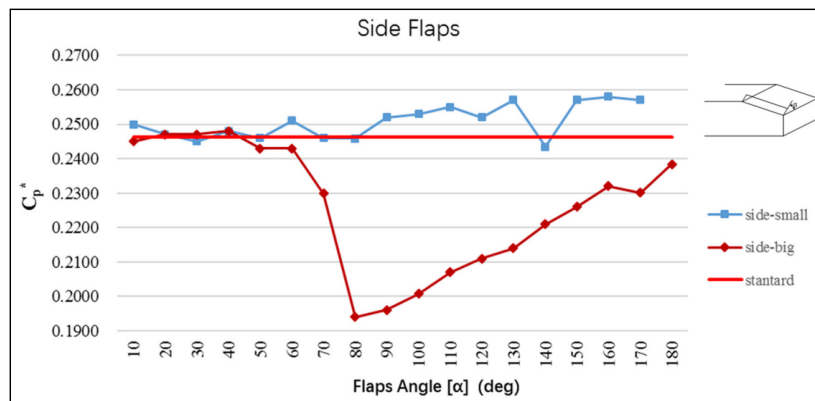


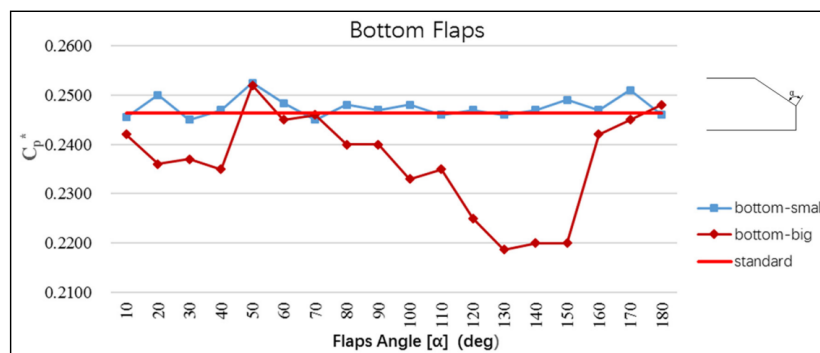
Fig - 5: Location of Flaps (a) Top, (b) Side, and (c) Bottom



(a) Top flaps drag results



(b) Side flaps drag results



(c) Bottom flaps drag results

Fig - 6: CFD drag generation findings for all three flaps with varying flap angles for Ahmed body with $\phi = 25^\circ$.
 Credit - Tian et al. [9], SAGE Publications Ltd., ([Creative Commons — Attribution 4.0 International — CC BY 4.0](https://creativecommons.org/licenses/by/4.0/)),
<https://doi.org/10.1177/1687814017711390>

Cheng and Mansor (2017) [10] numerically analyzed the simplified hatchback car model (i.e., Ahmed body with $\phi = 35^\circ$), to look at the effect of the pitch angle of the rear-roof spoiler at $-15^\circ, 0^\circ, 5^\circ, 10^\circ$, and 15° . The spoiler was 66.6 mm in length. Model and spoiler configurations are shown in fig—7 (a) & (b). CFD software ANSYS FLUENT 16 was used for all aerodynamic simulations via a “k-epsilon realizable model with enhanced wall treatment”. Figure 7(c) shows that depending on the pitch angle of the rear-roof spoiler, it may have a favorable or unfavorable influence on C_d . It has a positive impact at 0° and 5° pitch angles.

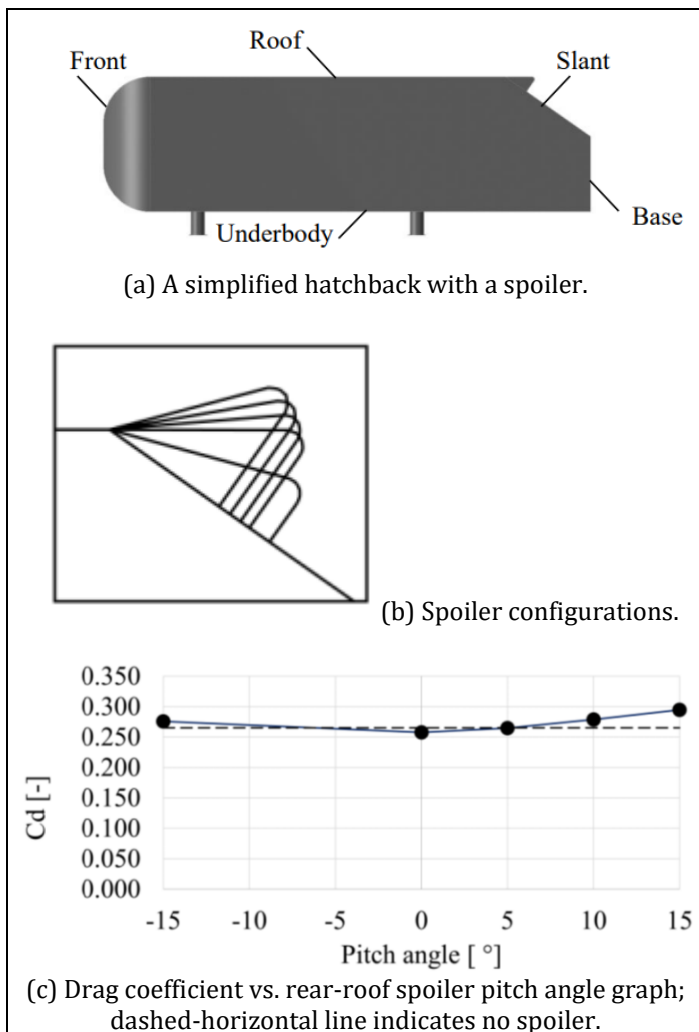


Fig - 7: Rear roof spoiler design and results.

Credit - Cheng and Mansor [10], IOP Publishing Ltd,

(Creative Commons — Attribution 3.0 Unported — CC BY 3.0),

<https://doi.org/10.1088/1742-6596/822/1/012008>

Viswanathan (2021) [11] used the CFD software ANSYS FLUENT version 19.1 via RANS-based models (i.e., Realizable k- ϵ , RNG k- ϵ , SST- k- ω) to analyze the aerodynamic behavior of multiple passive (VGs) installed on a conventional

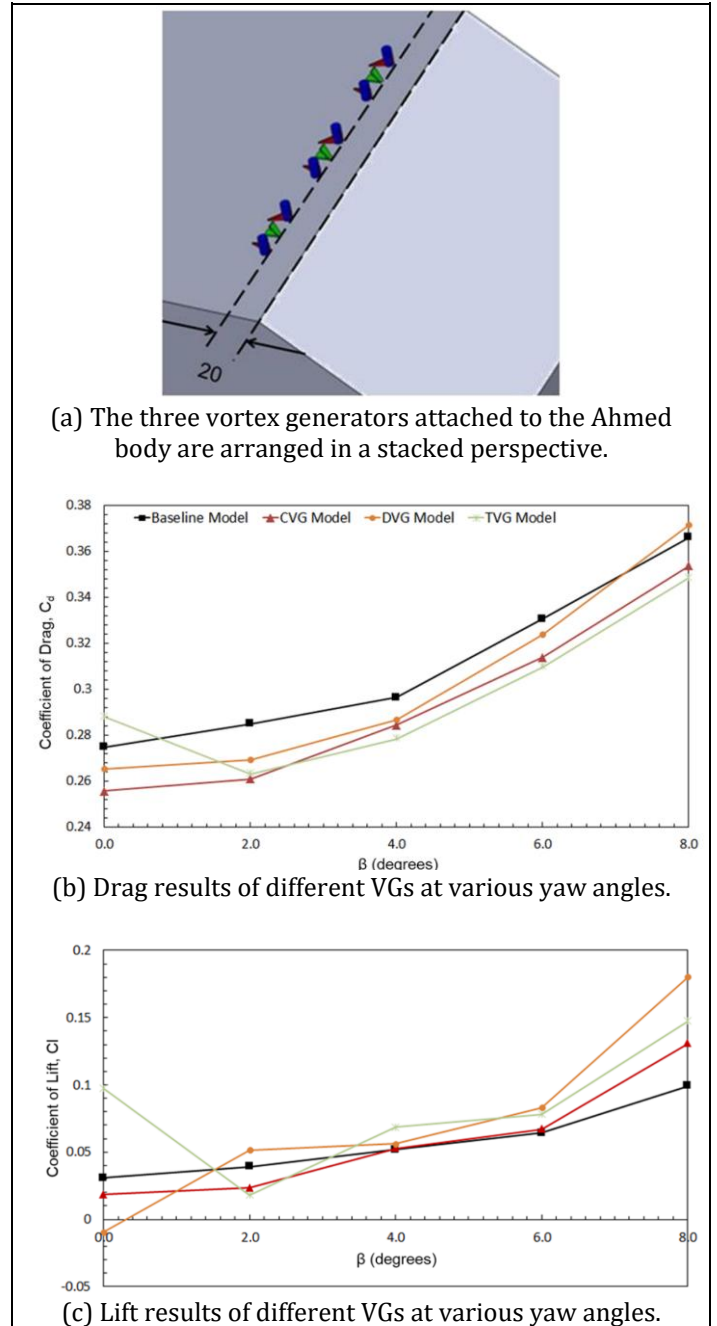


Fig - 8: VGs placement and results

Credit - Viswanathan [11], Springer Nature Switzerland AG, (Creative Commons — Attribution 4.0 International — CC BY 4.0),

<https://doi.org/10.1007/s40430-021-02850-8>

-Ahmed body with $\phi = 35^\circ$ and subjected to various yawing angles (β). The numerical results are rigorously verified using previously reported experimental results for the Ahmed body. Different VGs are added (see fig. 8a) to the verified model (i.e., delta-winglet, cylindrical, and trapezoidal). All simulations were analyzed for $\beta = 0^\circ$ to 8° with an increment of 2° . The inclusion of CVGs and DVGs

proves the aerodynamic performance for ($\beta=0^\circ$). On the other hand, the TVGs degrade performance by causing significant flow separation over the slant for ($\beta=0^\circ$). In smaller vehicle yawing situations, the proposed CVGs and TVGs look to be capable of reducing drag by up to 8.5 % and 7.7%, respectively. Drag and lift results of different VGs at various yaw angles are shown in fig. 8 (b) & (c), respectively.

3. CONCLUSION

This paper reviewed the aerodynamic drag reduction and its characteristics of an Ahmed body which is a simplified generic vehicle model for rear slant angles (φ) of 0° (a square back), 25° and 35° (a hatchback) using the CFD approach. Different types of ADD-ONS used in the previous studies are reviewed, such as porous layers, dimple grids based on the golf ball, V-shaped Riblets, VGs of hemispherical round roughness elements, flaps of different sizes, rear-roof spoilers and VGs of cylindrical, trapezoidal and delta shapes. The best ADD-ON for the square back configuration of Ahmed body was the dimple grid with the drag reduction of 36.5%, whereas for hatchback configuration ($\varphi = 25^\circ$) with side big flaps of angle 80° was the best with the drag reduction of 21%. For hatchback configuration ($\varphi = 35^\circ$), the best ADD-ON were combination of VGs attached on slant surfaces and V-shaped Riblets attached on rear surfaces with a drag reduction of 8.62%. All the study was numerically analyzed; none of them has experimentally analyzed the results. To compare flows, Particle image velocimetry (PIV) and CFD approaches should be deeply linked together. RANS simulations should be compared to PIV techniques [12].

- ✓ Modern artificial neural networks [13, 14] techniques can also be used to analyze the aerodynamic characteristics with better accuracy along with the CFD.

REFERENCES

- [1] Muhammad Nabil Farhan Kamal, Izuan Amin Ishak, Nofrizalidris Darlis, Daniel Syafiq Baharol Maji, Safra Liyana Sukiman, Razlin Abd Rashid, Muhamad Asri Azizul, A Review of Aerodynamics Influence on Various Car Model Geometry through CFD Techniques," *J. Adv. Res. Fluid Mech. Therm. Sci.*, vol. 88, no. 1, Oct. 2021, pp. 109–125.
- [2] W. M. Hamiga and W. B. Ciesielka, "Aeroacoustic Numerical Analysis of the Vehicle Model", *Appl. Sci.*, vol. 10, no. 24, Jan. 2020.
- [3] S.R. Ahmed, G. Ramm, and G. Faltin, "Some Salient Features Of The Time-Averaged Ground Vehicle Wake," in *the SAE international congress and exposition* (SAE Technical Paper, 1984), 840300.
- [4] V.Naveen Kumar, K. Lalit Narayan, L. N. V. Narasimha Rao and Y. Sri Ram, "Investigation of Drag and Lift Forces over the Profile of Car with Rears spoiler using CFD," *Int. J. Adv. Sci. Res.*, vol. 1, no. 8, Oct. 2015.
- [5] Alfadhel B. Kasim, Dr. Salah R. Al Zaidee, "Validation of Computational Fluid Dynamics Technique for Turbulent Wind Flow Approach, Bluff Two-Dimensional Body," *Int. J. Sci. Res.*, vol. 6, no. 4, April 2017, pp. 1361–1369.
- [6] Charles-Henri Bruneau, Patrick Gilli'eron and Iraj Mortazavi, "Passive Control Around the Two-Dimensional Square Back Ahmed Body Using Porous Devices," *J. Fluids Eng.*, vol. 130, no. 6, May 2008.
- [7] Mohd Faruq Abdul Latif, Muhammad Nur Othman, Qamar Fairuz Zahmani, Najiyah Safwa Khashi'ie, Beh Eik Zhen, Mohd Farid Ismail, Ahmad Yusuf Ismail, "Optimization of Boundary Layer Separation Reduction Induced by The Addition of a Dimple Grid on Top of a Bluff Body", *J. Adv. Res. Fluid Mech. Therm. Sci.*, vol. 64, no. 2, Dec. 2020, pp. 173–182.
- [8] X. Yang, Y. Hu, Z. Gong, J. Jian, and Z. Liu, "Numerical Study of Combined Drag Reduction Bases on Vortex Generators and Riblets for the Ahmed Body using IDDES Methodology", *J. Appl. Fluid Mech.*, vol. 15, no. 1, Jan. 2022, pp. 193–207.
- [9] J. Tian, Y. Zhang, H. Zhu, and H. Xiao, "Aerodynamic drag reduction and flow control of Ahmed body with flaps", *Adv. Mech. Eng.*, vol. 9, no. 7, Jul. 2017, 1687814017711390.
- [10] S Y Cheng and S Mansor 2017 *J. Phys.: Conf. Ser.* **822** 012008
- [11] H. Viswanathan, "Aerodynamic performance of several passive vortex generator configurations on an Ahmed body subjected to yaw angles", *J. Braz. Soc. Mech. Sci. Eng.*, vol. 43, no. 3, Feb. 2021, p. 131
- [12] F. Szodrai, "Quantitative Analysis of Drag Reduction Methods for Blunt Shaped Automobiles", *Appl. Sci.*, vol. 10, no. 12, Art. no. 12, Jan. 2020, 4313
- [13] D Yu Strelets et al 2021 *IOP Conf. Ser.: Mater. Sci. Eng.* **1024** 012115
- [14] Juliette Marrie, Pierre Baqu'e, Wouter Remmerie, Francesco Bardi, Pascal Fua, "Multi-fidelity optimization of a fixed-wing drone using Geometric Convolutional Neural Networks," January 29, 2020. <https://airshaper.com/research/deep-learning-automated-drone-design>